

## What is the Bond Dissociation Energy of the Vanadium Hydride Cation?

P. B. Armentrout\*

*Department of Chemistry, University of Utah, Salt Lake City, UT 84112, United States*

Yih-Chung Chang and Cheuk-Yiu Ng

*Department of Chemistry, University of California, Davis, CA 95616, United States*

**ABSTRACT:** Recent electronic state-selected measurements of the reactions of atomic vanadium cations with  $D_2$  and  $CO_2$  are reanalysed to properly account for the kinetic energy distribution of the reactant neutrals. The need for this is demonstrated in the present work by comparing the  $D_2$  data to that obtained previously in earlier experiments but unpublished. It is shown that the earlier data, which utilized a surface ionization source of  $V^+$ , and the state-selected data for  $V^+(a^5D_2)$  are essentially identical in the threshold regions where they overlap. Differences in the electronic state energies and kinetic energy distributions of  $V^+$  in the two experiments are very small and much smaller than the kinetic energy distribution of the neutral reactant, which is identical in both experiments. It is shown that properly accounting for the latter distribution alters the conclusions regarding the threshold energy for the endothermic formation of  $VD^+$  such that recent conclusions regarding the bond energy of  $VD^+$  are substantially altered, and found to reproduce the the original bond energy determination. Accounting for all experiments, a revised best value for  $D_0(VH^+)$  is  $2.07 \pm 0.09$  eV (or  $D_0(VD^+) = 2.10 \pm 0.09$  eV). This conclusion is validated by high-level *ab initio* calculations. Differences in the new and older data sets for the  $V^+ + D_2$  reaction at higher energies (above the onset for dissociation of the product ion) are also discussed. The same methodology is then applied to recent studies on the state-selected  $V^+ + CO_2$  reaction.

## INTRODUCTION

In 1985, Elkind and Armentrout (EA) examined the reaction of atomic vanadium cations ( $V^+$ ) with  $H_2$ ,  $HD$ , and  $D_2$  using a guided ion beam tandem mass spectrometer (GIBMS).<sup>1</sup> This was one of the earliest studies performed with this apparatus and the first in a series that examined how reaction cross sections changed as a function of both the kinetic energy and variations in the electronic state of the atomic transition metal cation.<sup>1-26</sup> In these studies, the electronic state of the metal cations was varied by utilizing two (sometimes more) ion sources: a) a surface ionization (SI) source in which atomic metal cations are emitted from a hot filament at a known temperature, and b) an electron ionization (EI) source in which energetic electrons ionize and dissociate a volatile compound containing the metal of interest. Using the SI source at  $2000 \pm 100$  K, which should yield a distribution of electronic states of  $83.3 \pm 1.4\%$   $^5D$ ,  $16.6 \pm 1.4\%$   $^5F$ , and  $0.14 \pm 0.04\%$   $^3F$ , EA obtained data for  $H_2$  and  $D_2$  that was analyzed to yield an average bond dissociation energy (BDE) for  $VH^+$  of  $2.05 \pm 0.06$  eV or for  $VD^+$  of  $2.08 \pm 0.06$  eV [after correcting for the zero point vibration energy (ZPVE) difference of  $0.03_1$  eV using calculated vibrational frequencies of  $1750$  and  $1250$   $cm^{-1}$ , respectively]. Recently, Xu, Chang, and Ng (XCN) have revisited this system (reaction with  $D_2$  only)<sup>27</sup> using a similar GIBMS apparatus but a refined metal cation source capable of generating ions in specific spin-orbit levels of multiple electronic states.<sup>28</sup> They observe the same overall behavior but interpret the threshold  $VD^+$  formation differently, obtaining the 0 K BDE,  $D_0(VD^+) = 2.5 \pm 0.2$  eV. As will be justified below, the purpose of this paper is to amend the threshold interpretation of XCN by properly accounting for the kinetic energy distribution of the neutral  $D_2$  reactant, so-called “Doppler broadening”. The need for this treatment is detailed, the threshold of the recent experiments reevaluated, and high-level *ab initio* calculations are used to bolster the threshold assignment made previously and in the present work. The results are then extended to reexamine the state-selected studies of the reactions of  $V^+$  with  $CO_2$ .<sup>29</sup>

## EXPERIMENTAL AND THEORETICAL METHODS

The experimental details of both the earlier work of Elkind and Armentrout and the recent studies of Ng and coworkers are provided in the original papers.<sup>1, 27, 29</sup> For the theoretical calculations conducted here of both VH and VH<sup>+</sup>, we used Gaussian16<sup>30</sup> and optimized geometries at the MP2/aug-cc-pV(Q+d)Z level of theory. Single point energies were then calculated at the CCSD(T)/CBS level, where the complete basis set (CBS) extrapolations used aug-cc-pV(X+d)Z basis sets with X = Q and 5 and were formulated using the method described by Halkier et al.<sup>31-34</sup> for both Hartree-Fock energies and CCSD(T) correlation energies.

## RESULTS AND DISCUSSION

### *Reaction of V<sup>+</sup> + D<sub>2</sub>: Threshold Region*

To evaluate the need for reassessing the threshold assignment of XCN, it is useful to quantitatively compare the early and more recent kinetic-energy dependent integral cross section ( $\sigma$ ) measurements of the V<sup>+</sup> + D<sub>2</sub> reactions. XCN compared their results for V<sup>+</sup>(*a*<sup>5</sup>D<sub>2</sub>) + D<sub>2</sub> with the published data of EA for V<sup>+</sup>(SI) + H<sub>2</sub>, noting that “Although it was asserted that the observed  $\sigma$  values of V<sup>+</sup> + H<sub>2</sub> were similar to those of V<sup>+</sup> + D<sub>2</sub>, no experimental  $\sigma$  measurements for the V<sup>+</sup> + D<sub>2</sub> data reaction were reported previously.” Here, we rectify this omission by showing in Figure 1 the original data of EA for both reactions along with that from XCN. In order to emphasize the comparison of the energy dependence rather than the absolute magnitudes, we have scaled the data of XCN down slightly (by 30%, well within their stated absolute uncertainty of  $\leq 50\%$ ) and we have scaled the D<sub>2</sub> data of EA up by 30% (well within the combined uncertainties in the absolute magnitudes of 20% each). First, we point out the agreement between the H<sub>2</sub> and D<sub>2</sub> data from EA, hopefully justifying the previous “assertion” that the data are similar. Second, very careful comparison of these two data sets shows that the D<sub>2</sub> cross sections lag slightly behind those for H<sub>2</sub>, consistent with the expectation from ZPVE differences that the D<sub>2</sub> reaction has a higher threshold by 0.05 eV. Third, as noted by XCN, the comparison shows “fair agreement, except for the peak positions and peak widths.” Here, we augment this description by pointing out that the

shape of all three cross sections is the same in the threshold region. The differences at higher energies are discussed further below, but for the moment, we concentrate on the key threshold region, as this determines the BDE value obtained.

We can first ask the question of why the data are so similar, given that the data from XCN has the spin-orbit state of  $V^+$  chosen precisely (in Figure 1, it's the  $a^5D_2$  level at  $106.6 \text{ cm}^{-1} = 0.013 \text{ eV}$  above the ground  $a^5D_0$  level), whereas the data from EA “involved no  $J$ -state selections, and the quantitative quantum state distributions were unclear” according to XCN. This characterization is inaccurate in that EA specifically state that the SI source should yield a thermal distribution of electronic states at the temperature of the SI filament ( $2000 \pm 100 \text{ K}$  in these experiments), which therefore can provide the detailed distribution of all spin-orbit levels. It can be argued that this assumption has never been rigorously proven (or disproven), but the SI filament temperature dependence of endothermic reactions has been studied many times and also compared with results using thermalized flow tube sources.<sup>2, 4, 7, 9, 11-14, 16-18, 20-21, 24</sup> The results of these studies are all found to be consistent with this assumption, which has also been independently confirmed for the case of  $Co^+$ .<sup>35</sup> Further, as shown below, the state-selected measurements of the  $V^+ + D_2$  reactions can be used to reproduce the earlier  $V^+(SI) + D_2$  cross sections and similarly, state-selected  $V^+ + CH_4$  reaction results can be used to reproduce earlier  $V^+(SI) + CH_4$  cross sections<sup>7</sup> (including the temperature dependence) with fidelity. The latter two results are probably the best demonstration yet that the equilibrium assumption is correct.

Given this assumption, the average electronic energy ( $E_{el}$ ) of the  $V^+(SI)$  ions in the study of EA is  $0.082 \pm 0.005 \text{ eV}$ , such that these ions should have  $0.07 \text{ eV}$  more energy than  $V^+(a^5D_2)$ . However, XCN determine that the  $a^5F$  state of  $V^+$  is about an order of magnitude less reactive than the ground  $a^5D$  state and the  $a^3F$  state is about seven times more reactive. Further, the probability of reaction has no dependence on  $J$ -levels within these individual electronic manifolds of the  $a^5D$ ,  $a^5F$ , and  $a^3F$  states. If we take this new information into account, then the weighted  $E_{el}$  of  $V^+(SI) = 0.043 \pm 0.005 \text{ eV}$ . Thus, the two experiments have  $V^+$  electronic energies with differences that are very small ( $\sim 0.03 \text{ eV}$ ) and clearly cannot influence the results obtained significantly.

Furthermore, both EA and XCN correct their measured thresholds (called  $\Delta E$  by XCN) by the perceived electronic energy and also by the rotational energy of the reactant neutral  $D_2$  ( $E_{\text{rot}} = 0.026$  eV as both experiments have room temperature gas cells where the vibrational energy contribution is negligible). Once these energies are included EA refer to the threshold for reaction as  $E_0$ , the threshold in the absence of internal energy distributions (i.e., at 0 K). Both studies also obtain the final BDEs by using eq 1 (or the  $H_2$  analogue for EA).

$$D_0(V^+-D) = D_0(D_2) - E_{\text{el}} - E_{\text{rot}} - \Delta E = D_0(D_2) - E_0 \quad (1)$$

According to eq 1, the accurate determination of  $D_0(V^+-D)$  requires the precise measurement of the threshold energy  $\Delta E$  at 0 K. The application of the newly developed single spin-orbit state selection scheme along with the supersonic cooling of  $V^+$  ions should facilitate the 0 K  $\Delta E$ -threshold assignment because  $E_{\text{el}}$  is exactly defined and the supersonic expansion  $V^+$  source reduces this reactant's kinetic-energy distribution. Given the similarity in the data and the very small differences in  $E_{\text{el}}$ , it should have been expected that that similar threshold energies and similar BDEs would result, yet XCN find a difference of  $\approx 0.4$  eV. This discrepancy is a result of how the threshold energies were assigned in both experiments. XCN originally used an “onset of observable signal” (OOS) criterion, finding their first  $VD^+$  signal at  $\Delta E = 2.0$  eV for the  $a^5D_2$  level ( $E_{\text{el}} = 0.013$  eV),  $\Delta E = 1.7$  eV for the  $a^5F_1$  level ( $E_{\text{el}} = 0.323$  eV), and  $\Delta E = 0.8$  eV for the  $a^3F_2$  level ( $E_{\text{el}} = 1.071$  eV).<sup>36</sup> For all three thresholds, they assign an uncertainty of  $\pm 0.1$  eV because they collect points every 0.1 eV in the threshold regions. Given  $D_0(D_2) = 4.556$  eV,<sup>37-38</sup> using these three threshold energies in eq 1 leads to  $D_0(V^+-D)$  values of 2.52, 2.51, and  $2.66 \pm 0.1$  eV, respectively. The average of these led to their final suggested value of  $2.56 \pm 0.2$  eV (two standard deviations).

In contrast, EA took advantage of the seminal work by Chantry in 1971 on “Doppler Broadening in Beam Experiments” where he showed that the thermal motion of the neutral gas contributes a large distribution to the energy available to the reaction system.<sup>39</sup> Chantry dubbed this “Doppler Broadening” because the neutrals moving towards the ions lead to much higher relative energies, whereas those moving away have much lower energies than the mean. His

interpretation has been validated by many experiments in the interim. This broadening is particularly severe in the present case because  $\text{H}_2$  and  $\text{D}_2$  are light molecules having high velocities. The effect of this broadening is easily seen in the data of Figure 1 as the curvature in the threshold region of all three cross sections. Shown below the baseline are the Doppler distributions for the  $\text{D}_2$  reaction at 2.0, 4.5, and 8.0 eV, which have full-widths at half maximum (FWHMs) of 0.73, 1.09, and 1.46 eV. It can be seen that this distribution at 2 eV matches the curvature in the threshold region.

A simple demonstration that the kinetic energy distribution of the neutral molecules needs to be included in the threshold determination can be performed by changing the temperature of the neutral gas. If the OOS criterion were correct, then the threshold would not change with this temperature, whereas if Chantry is correct, the OOS position would change with temperature, but properly accounting for the change in temperature would provide the same 0 K threshold energy. In this regard, a study by Sunderlin and Armentrout of the  $\text{C}^+$  and  $\text{N}^+$  reactions with  $\text{H}_2$ , HD, and  $\text{D}_2$  shows conclusively that the cross sections change in exactly the manner anticipated by Chantry when the temperature of the neutral reagent changes (in that study, from 305 to 105 K).<sup>40</sup> Notably, Chantry's result was later extended by Lifshitz et al. to include the kinetic energy distribution of the ions in the data analysis.<sup>41</sup> For the  $\text{V}^+ + \text{D}_2$  reactions, EA had a kinetic energy distribution of their  $\text{V}^+$  ions with a FWHM of 0.7 eV, whereas the supersonic  $\text{V}^+$  source of XCN had a narrower distribution of 0.2 eV, both in the laboratory frame. When converted to the center-of-mass frame, these distributions have FWHMs of 0.051 and 0.015 eV, respectively, for the  $\text{D}_2$  reaction (0.026 and 0.008 eV for the  $\text{H}_2$  reaction). When convolved with the broad kinetic energy distribution of the  $\text{D}_2$  neutral, these ion energy distributions introduce a negligible change and are inconsequential in the data analysis. For example, at 2.0 eV, the Doppler broadening has a FWHM of 0.727 eV, and when the kinetic energy distributions of  $\text{V}^+$  are included, the FWHM becomes 0.729 eV for EA and 0.727 eV for XCN in the center-of-mass frame.

As Chantry originally demonstrated, the proper way to handle this distribution is to convolve a model with the distribution and then compare that with the data, the procedure used by

EA and used below. The problem is what model to use because there is no rigorous theory for the shape of a reaction cross section as a function of kinetic energy. At the time the original  $V^+ + H_2$ , HD,  $D_2$  study was published, the best form for an appropriate model was still being tested and developed, but most approaches used in the literature have centered around a shape defined by eq 2,<sup>42-45</sup>

$$\sigma(E) = \sigma_0 (E + E_{el} + E_{int} - E_0)^n / E^m \quad (2)$$

the modified line-of-centers (MLOC) model, where the simple LOC model dictates that the parameters  $n$  and  $m$  equal unity. As noted above, the energy available includes that in translation ( $E$ ) in the center-of-mass frame, internal energy of the neutral reactant ( $E_{int}$ , exclusively rotation for  $H_2$  and  $D_2$ ), and the atomic reactant ion ( $E_{el}$ ). EA tested many forms of this equation and found that three worked particularly well in reproducing the data: LOC ( $n = m = 1$ ),  $n = m$  (allowed to vary),  $n$  (allowed to vary) and  $m = 1$ . In the intervening years, the Armentrout group has settled on the latter model,<sup>46-47</sup> originally designed to describe translationally driven reactions,<sup>45</sup> as most appropriate for the kinetic energy dependent systems studied by GIBMS. Ultimately, any of these approaches yields similar results and appropriate uncertainties in this method are handled by measuring multiple data sets (11 each in the study of EA) along with variations in  $n$  as well as the uncertainties in  $E_{el}$ ,  $E_{int}$ , and the absolute kinetic energies.

The results of this type of modeling are shown in Figure 2 for the  $H_2$  reaction cross section. Table 1 lists the parameters used in eq 1 to reproduce both the  $H_2$  and  $D_2$  data of EA. Models assuming equal reactivity for all  $V^+$  electronic states, as assumed by EA, are shown in red in Figure 2 and relative factors of 1.0 : 0.1 : 7.0 for the  $a^5D$ ,  $a^5F$ , and  $a^3F$  states, as found by XCN, are shown in blue in Figure 2 and parameters for both are listed in Table 1. The latter assumption raises the  $E_0$  threshold energies by only 0.01 eV because the cross sections remain dominated by the  $a^5D$  state. Figure 2 shows that the MLOC model, after convolution over the kinetic energy distributions of both reactants and the electronic energy distribution of the  $V^+(SI)$  reactant, reproduces all the data faithfully down into the noise of the earlier experiments. Notably, enhancing the reactivity of the  $a^3F$  state as found by XCN reproduces the small “tail” in the SI data very well (also evident in

the  $D_2$  data). Considering that the  $a^3F$  accounts for only  $0.0014 \pm 0.0004$  of the ions present at 2000 K, the sensitivity of the experiment is evident. This result simultaneously corroborates the relative state-selected reactivities found by XCN and the assumption of thermal equilibrium of spin-orbit levels by EA. The dashed lines exclude these distributions, and their onset ( $E_0$ ) represents the true threshold energy according to the MLOC model. The average of all determinations of the  $V^+(SI) + H_2$  and  $D_2$  data of EA after correction for ZPVE gives a 0 K BDE for  $VH^+$  of  $2.04 \pm 0.07$  eV (two standard deviations of the mean), reproducing the value reported by EA.

It can be realized that the modeling approach that properly incorporates Doppler broadening provides a more precise means of determining the threshold as it relies on accurately reproducing not just the OOS, but the entire cross section curve. The observation that such a simple model, when properly convolved, reproduces the experimental data with such fidelity, Figure 2, suggests the legitimacy of this approach.

This conclusion is amplified by reanalyzing the data obtained by XCN for reactions of  $D_2$  with  $V^+$  in its  $a^5D_2$ ,  $a^5F_1$ , and  $a^3F_2$  levels. Figure 3 shows this analysis including the kinetic energy distribution of the  $D_2$  reactant. Notably, because there are fewer points in these data sets, the parameter  $n$  in eq 2 was constrained to values close to those determined from the data of EA (and close to unity, as appropriate for the simple LOC model). It can be seen that the reproduction of the data for all three states is very good in the threshold region up to the peak cross section in each case. Furthermore, onsets of the dashed lines (which do not include the kinetic energy distributions of either reactant) are separated by energies nearly equivalent to the known excitation energies,  $E_{el}$ , shown by the arrows. The parameters of eq 2 used in these analyses are also included in Table 1. It can be seen that the thresholds for all three state-selected experiments are in excellent agreement with the values obtained for the EA data ( $D_2$  reaction). After correction for ZPVEs, the weighted average of the three experiments of XCN yields a  $VH^+$  BDE at 0 K of  $2.10 \pm 0.06$  eV (two standard deviations of the mean). A weighted average of all experiments provides a  $VH^+$



BDE of  $2.07 \pm 0.09$  eV, which we believe is the best experimental value available. ZPVE adjustments yield a best value of  $2.10 \pm 0.09$  eV for  $D_0(V^+-D)$ .

### *VH and Theoretical Results*

In their discussion of the discrepancy between their newly derived value for  $D_0(V^+-D)$  and that from EA, XCN also mention the neutral BDE, which Cheng et al. have recently reported as  $D_0(VH) = 2.31 \pm 0.07$  eV.<sup>48</sup> This value revised the original determination of Chen, Clemmer, and Armentrout of  $2.13 \pm 0.07$  eV determined from reaction 3 with  $RH = HN(CH_3)_2$  and  $N(CH_3)_3$ .<sup>49</sup>



What Cheng et al. (and independently, Fang et al.<sup>50</sup>) pointed out was that the neutral thermochemistry in the literature had evolved in the interim (in this case, the values of  $D_0(R^+-H^-)$  of the two amines used in reaction 3). Using the *original* threshold measurements along with new values for  $D_0(R^+-H^-)$ , the corrected experimental value for  $D_0(VH)$  of  $2.31 \pm 0.07$  eV was obtained. This value is in good agreement with high-level *ab initio* calculations yielding 2.41 and 2.39 eV.<sup>48</sup> <sup>50</sup> XCN then cited a thermodynamic cycle that relies on the ionization energies (IEs) of V (well-known experimentally) and VD (an uncited theoretical value) with a difference of 0.184 eV, such that  $D_0(VD) = D_0(V^+-D) + 0.184$  eV. They pointed out that given the revised BDE of VD, incorrectly equated with  $D_0(VH) = 2.31 \pm 0.07$  eV, the value for  $D_0(V^+-D)$  should be  $2.13 \pm 0.07$  eV. If we properly correct for ZPVE effects (using vibrational frequencies for VH of  $1635\text{ cm}^{-1}$  and for VD of  $1168\text{ cm}^{-1}$  calculated here at the MP2/aug-cc-pV(5+d)Z level), this thermodynamic cycle converts  $D_0(VD) = 2.34 \pm 0.07$  eV to  $D_0(V^+-D) = 2.16 \pm 0.07$  eV, which agrees nicely with the directly measured value from EA,  $2.08 \pm 0.06$  eV (again corrected for ZPVE), the revised value obtained above for XCN,  $2.13 \pm 0.06$  eV, and the best value of  $2.10 \pm 0.09$  eV. This agreement is in accord with mean absolute deviations of 0.09 and 0.06 eV between these theoretical results compared with experimental results for 20 transition metal diatomics.<sup>48, 50</sup>

To provide additional context to the thermochemistry of VH and  $VH^+$ , we examined these species theoretically. Geometries for the VH ( $^5\Delta$ ) and  $VH^+$  ( $^4\Delta$ ) ground states were determined at

the MP2/aug-cc-pV(Q+d)Z level yielding bond lengths of 1.689 and 1.655 Å, respectively. Once extrapolated to the CBS limit, the BDEs are 2.30 and 2.17 eV, respectively. More refined calculations obtained using the same CCSD(T) computational protocol as that used for the calculations of VH in Ref. 49 were also conducted by our collaborator L. Cheng. He obtained IEs for V and VH of 6.749 eV (compared to the experimental value of 6.746187 eV<sup>36</sup>) and 6.962 eV, for a difference of 0.216 eV. This difference is similar to the theoretical value cited by XCN (0.184 eV), and most importantly, matches the experimental differences between  $D_0(\text{VH}) = 2.31 \pm 0.07$  eV and  $D_0(\text{V}^+\text{-H})$ ,  $0.27 \pm 0.09$  (EA),  $0.21 \pm 0.09$  (XCN revised), and  $0.24 \pm 0.11$  eV (best). When combined with the theoretical value  $D_0(\text{VH}) = 2.41$  eV,<sup>31</sup> the theoretical difference of 0.216 eV leads to  $D_0(\text{V}^+\text{-H}) = 2.19$  eV, in agreement with the CCSD(T)/CBS value of 2.17 eV obtained here and in reasonable agreement with the experimental values of  $2.05 \pm 0.06$  (EA),  $2.12 \pm 0.07$  (revised XCN), and  $2.08 \pm 0.11$  (best) eV (all with similar discrepancies as for VH).

#### *Reaction of $\text{V}^+ + \text{D}_2$ : High-energy Region*

We now return to the overall shape of the cross sections at higher energies, where there are more severe discrepancies between the data of EA and XCN, Figure 1. XCN suggested that the “difference in peak width may be accounted for by the different kinetic energy resolutions and quantum electronic state purities or reactant  $\text{V}^+$  ions prepared by different schemes.” In contrast, as demonstrated above, the electronic state purity has a negligible effect on the average energy (0.03 eV difference) as does the kinetic energy distribution of the  $\text{V}^+$  ions (0.04 eV difference). Rather, the energy distributions are dominated by the motion of the neutral reactant, which is identical in the experiments of EA and XCN. (Note too that the FWHM of the kinetic energy distribution at 4.5 eV is 1.09 eV for  $\text{D}_2$  and 1.11 eV for  $\text{H}_2$ , i.e., essentially identical. These FWHM values are perturbed by  $<0.01$  eV by including the kinetic and electronic energy distributions of  $\text{V}^+$ .)

Ultimately, both EA and XCN agree that the reason the  $\text{VD}^+$  (and  $\text{VH}^+$ ) cross section reaches a maximum is that the product can decompose beginning at the point where the  $\text{V}^+ + \text{D} +$

D channel can open, i.e., beginning at  $D_0(D_2) = 4.556$  eV (4.478 eV for  $H_2$ ).<sup>37, 51</sup> So what does explain the difference in behavior? To answer this question, we return to modeling the cross sections appropriately convolved with all energy distributions. This is shown in Figure 4 for both  $VH^+$  and  $VD^+$ . Here, in addition to the MLOC model of eq 2, we have included a model for the probability of dissociation of the  $VH^+$  ( $VD^+$ ) product,  $P_D$ .<sup>52</sup> This model is controlled by two parameters:  $E_D$ , the energy at which the decomposition can begin, and  $p$ , which like  $n$  in eq 2, controls the shape of the cross section. This model, which includes contributions of angular momentum conservation (which takes into account having to overcome the centrifugal barrier for molecules having rotational energy),<sup>53</sup> was developed shortly after the publication by EA and was not included there. Nevertheless, Figure 4 shows that it reproduces the behavior of the  $VH^+$  and  $VD^+$  cross sections throughout the threshold regions, through the peaks, and up to about 6 or 7 eV. Notably,  $E_D$  was fixed at  $D_0(H_2) = 4.478$  eV or  $D_0(D_2) = 4.556$  eV (and  $p = 1$ ) in the models shown. Clearly, this simple model not only reproduces each individual data set, it also reproduces the differences between them, which are partly attributable to the larger BDE of  $D_2$ . Further, the  $VD^+$  cross section declines more slowly because the heavier D atom can carry away more energy than the lighter H atom. At higher energies (above 6 or 7 eV or so), it is believed that the collisions between  $V^+$  and  $H_2$  ( $D_2$ ) become increasingly impulsive and the probability of forming the  $VH^+$  ( $VD^+$ ) molecule decreases more rapidly. Indeed, when both sets of data are viewed on a log-log scale (Figure 2), it can be seen that the slope of the decline increases at these energies, indicating a change in the mechanism (or possibly incomplete collection of products at such high energies). In any event, the model shows that using the correct thermodynamics for dissociation of the  $VH^+$  ( $VD^+$ ) product leads to an accurate description of the experimental cross sections of EA over an extended energy range.

The same model can be successfully applied to the XCN data for the  $a^5F_1$  and  $a^3F_2$  levels, which have  $E_{el} = 0.323$  and 1.071 eV, respectively, such that the peak in the cross section should come at lower collision energies, specifically,  $E_D = D_0(D_2) - E_{el} = 4.23$  and 3.48 eV, respectively. As shown in Figure 3, the MLOC model that includes  $P_D$  and these values of  $E_D$  reproduces the

$a^5F_1$  and  $a^3F_2$  data throughout the threshold regions, the peaks in the cross section, and the initial declines in the cross sections associated with dissociation. Deviations occur at higher energies, presumably for the same reasons as the EA data. Notably, the peaks in the cross sections for  $a^5F_1$  and  $a^3F_2$  are distributed according to  $E_{el}$ , like the threshold energies, but this is not true for the  $a^5D_2$  cross section. In contrast to the data of EA, the data of XCN for  $a^5D_2$  begins to decline sharply beginning at 4.0 eV, well before it is thermodynamically possible to undergo dissociation. Despite careful tuning of the ion lenses and bias applied to the analysis quadrupole mass filter, it is possible that the products were not collected efficiently at high energies in this experiment. In this regard, the rf octopole technology used by both groups generally provides efficient product collection but is *not* a panacea.

#### *Reaction of $V^+ + CO_2$*

Chang, Xu, and Ng (CXN) examined the state-selected reactions of  $V^+$  with  $CO_2$ , observing both  $VO^+$  and  $VCO^+$  channels.<sup>29</sup> The results obtained were generally in agreement with the previous work of Sievers and Armentrout (SA) on the same reaction, where  $V^+$  ions were generated using a direct current discharge/flow tube (DC/FT) source that was shown to generate ions exclusively in their  $^5D$  ground state.<sup>54</sup> It was assumed that the spin-orbit levels were populated according to a Maxwell-Boltzmann distribution at the temperature of the flow gases (90:10% He:Ar), 300 K. This would provide a distribution of J levels for 0, 1, 2, 3, and 4 of 9.2, 23.2, 27.6, 23.7, and 16.3%, respectively, with no population of higher lying states. The average electronic energy of this distribution is 0.018 eV, similar to that for  $a^5D_2$  (0.013 eV). The FWHM of the vanadium ion kinetic energy distribution was 0.25 – 0.40 eV in the laboratory frame, or 0.12 – 0.19 eV in the CM frame, compared to 0.09 eV in the CM frame in the experiments of CXN. Compared with the Doppler broadening, which is the same in both experiments, both of these differences are negligible.

The reaction of  $V^+$  with  $CO_2$  to form  $VO^+ + CO$  is exothermic for all electronic states of  $V^+$ , consistent with the observations in both studies of no barriers to formation of these products

no matter how the ions were generated. In contrast, reaction to form  $\text{VCO}^+ + \text{O}$  is strongly endothermic with an apparent threshold near 4 eV for  $\text{V}^+(a^5D_2)$  and  $\text{V}^+(\text{DC/FT})$ . The state-selected study assigned OOS thresholds of 4.1, 3.8, and  $3.0 \pm 0.1$  eV for reactions of the  $a^5D_2$ ,  $a^5F_1$ , and  $a^3F_2$  levels. It was pointed out that these are consistent with the known thermochemical threshold, although this was not specified very precisely. The best value for  $D_0(\text{V}^+-\text{CO})$ ,  $1.17 \pm 0.03$  eV, comes from a direct collision-induced measurement of Sievers and Armentrout,<sup>55</sup> published slightly after their study of the  $\text{V}^+ + \text{CO}_2$  reaction (although the value was cited by SA and also used by CXN). After correcting for the electronic excitation energies, and using  $D_0(\text{O}-\text{CO}) = 5.453 \pm 0.001$  eV,<sup>38</sup> the threshold energies for the three  $\text{V}^+$  levels should be 4.27, 3.96, and  $3.21 \pm 0.03$  eV, respectively, slightly *above* the assigned OOS thresholds. In contrast, when SA analyzed their data, properly accounting for the Doppler broadening, they obtained a threshold of  $E_0 = 4.59 \pm 0.30$  eV, whereas the thermodynamic threshold of  $4.28 \pm 0.03$  eV is slightly *below* that. Note that the difference between the assigned thresholds for  $\text{V}^+(a^5D_2)$  and  $\text{V}^+(\text{DC/FT})$  is 0.5 eV, consistent with the Doppler broadening of 0.81 eV (FWHM) at 4.3 eV in this system. In this case, we believe that the threshold obtained for  $\text{VCO}^+ + \text{O}$  formation is an unreliable indicator of the thermochemistry because of the direct competition with the much more favorable formation of  $\text{VO}^+ + \text{CO}$ , which is over an order of magnitude larger at about 5 eV in both studies. As originally pointed out by SA, both reactions involve cleavage of the O-CO bond and therefore directly compete. This competition should shift the threshold for the less favorable reaction (here,  $\text{VCO}^+ + \text{O}$ ) to higher energies, as found by the threshold analysis of SA.

CXN directly compared the cross sections obtained for reactions of  $\text{CO}_2$  with  $\text{V}^+(a^5D_2)$  and  $\text{V}^+(\text{DC/FT})$ . Both cross sections exhibit the same curvature and absolute magnitude from the apparent thresholds of  $\sim 4$  eV up to 5 eV. Hence, a proper analysis of these cross sections or those for  $\text{V}^+(a^5F_1)$  and  $\text{V}^+(a^3F_2)$  should reproduce the threshold result obtained by SA. Above 5 eV, the cross sections differed appreciably. Those for SA continue to increase and then decline slowly at higher energies, compared to a precipitous decline in the data of CXN.

## CONCLUSION

As demonstrated above, properly accounting for the kinetic energy distribution of the reactant neutral alters the threshold determinations made in recent state-specific reactions of vanadium cations with  $D_2$  and  $CO_2$ . As detailed above and confirmed by high-level *ab initio* calculations, the previously determined value for  $D_0(V^+-H)$  of  $2.05 \pm 0.06$  eV now agrees with a reevaluated determination of  $2.10 \pm 0.06$  eV for the data of XCN. A best value of  $2.07 \pm 0.09$  eV is determined from a combination of both experiments. In the  $CO_2$  system, thresholds for production of  $VCO^+ + O$  are consistent in both experiments and should lie slightly above the true thermodynamic threshold because of direct competition with the dominant formation of  $VO^+ + CO$ . Because the data analysis does not account for this competition, accurate thermodynamic conclusions cannot be drawn from determinations of this threshold.

## Acknowledgement

This work is supported by the National Science Foundation, Grant CHE-1664618 (PBA) and CHE-1763319 (CYN). PBA thanks Prof. Lan Cheng for graciously performing new calculations on the ionization energy of VH that are cited here and the Center for High Performance Computing at the University of Utah for a generous allocation of computer time. CYN is also grateful to Dr. Huie Tarnng Liou for his generous donation of research support for the Ng Laboratory.

## AUTHOR INFORMATION

Corresponding Author

\*E-mail: armentrout@chem.utah.edu

ORCID

P. B. Armentrout: 0000-0003-2953-6039

Cheuk-Yiu Ng: 0000-0003-4425-5307

## References

1. Elkind, J. L.; Armentrout, P. B., Effect of Kinetic and Electronic Energy on the Reaction of  $V^+$  with  $H_2$ , HD and  $D_2$ . *J. Phys. Chem.* **1985**, *89*, 5626-5636.
2. Elkind, J. L.; Armentrout, P. B., Effect of Kinetic and Electronic Energy on the Reactions of  $Fe^+$  with  $H_2$ , HD and  $D_2$ : State-Specific Cross Sections for  $Fe^+(^6D)$  and  $Fe^+(^4F)$ . *J. Phys. Chem.* **1986**, *90*, 5736-5745.
3. Elkind, J. L.; Armentrout, P. B., Effect of Kinetic and Electronic Energy on the Reactions of  $Mn^+$  with  $H_2$ , HD and  $D_2$ . *J. Chem. Phys.* **1986**, *84*, 4862-4871.
4. Elkind, J. L.; Armentrout, P. B., Effect of Kinetic and Electronic Energy on the Reactions of  $Co^+$ ,  $Ni^+$  and  $Cu^+$  with  $H_2$ , HD and  $D_2$ . *J. Phys. Chem.* **1986**, *90*, 6576-6586.
5. Elkind, J. L.; Armentrout, P. B., State-specific Reactions of Atomic Transition Metal Ions with  $H_2$ , HD and  $D_2$ : Effects of d Orbitals on Chemistry. *J. Phys. Chem.* **1987**, *91*, 2037-2045.
6. Elkind, J. L.; Armentrout, P. B., Effect of Kinetic and Electronic Energy on the Reactions of  $Cr^+$  with  $H_2$ , HD and  $D_2$ . *J. Chem. Phys.* **1987**, *86*, 1868-1877.
7. Aristov, N.; Armentrout, P. B., Methane Activation by  $V^+$ : Electronic and Translational Energy Dependence. *J. Phys. Chem.* **1987**, *91*, 6178-6188.
8. Elkind, J. L.; Armentrout, P. B., Effect of Kinetic and Electronic Energy on the Reactions of  $Ti^+$  with  $H_2$ , HD and  $D_2$ . *Int. J. Mass Spectrom. Ion Processes* **1988**, *83*, 259-284.
9. Schultz, R. H.; Elkind, J. L.; Armentrout, P. B., Electronic Effects in C-H and C-C Bond Activation: State-specific Reactions of  $Fe^+(^6D, ^4F)$  with Methane, Ethane and Propane. *J. Am. Chem. Soc.* **1988**, *110*, 411-423.
10. Georgiadis, R.; Armentrout, P. B., Translational and Electronic Energy Dependence of Chromium Ion Reactions with Methane. *J. Phys. Chem.* **1988**, *92*, 7067-7074.
11. Sunderlin, L. S.; Armentrout, P. B., Methane Activation by  $Ti^+$ : Electronic and Translational Energy Dependence. *J. Phys. Chem.* **1988**, *92*, 1209-1219.
12. Armentrout, P. B., Electronic State-Specific Transition Metal Ion Chemistry. *Annu. Rev. Phys. Chem.* **1990**, *41*, 313-344.
13. Clemmer, D. E.; Sunderlin, L. S.; Armentrout, P. B., Ammonia Activation by  $V^+$ : Electronic and Translational Energy Dependence. *J. Phys. Chem.* **1990**, *94* (1), 208-217.
14. Clemmer, D. E.; Sunderlin, L. S.; Armentrout, P. B., Ammonia Activation by  $Sc^+$  and  $Ti^+$ : Electronic and Translational Energy Dependence. *J. Phys. Chem.* **1990**, *94* (7), 3008-3015.
15. Fisher, E. R.; Armentrout, P. B., Electronic Effects in C-H and C-C Bond Activation: Reactions of Excited State  $Cr^+$  with Propane, Butane, Methylpropane, and Dimethylpropane. *J. Am. Chem. Soc.* **1992**, *114*, 2049-2055.
16. Chen, Y.-M.; Clemmer, D. E.; Armentrout, P. B., Kinetic and Electronic Energy Dependence of the Reactions of  $Sc^+$  and  $Ti^+$  with  $D_2O$ . *J. Phys. Chem.* **1994**, *98*, 11490-11498.
17. Clemmer, D. E.; Chen, Y.-M.; Aristov, N.; Armentrout, P. B., Kinetic and Electronic Energy Dependence of the Reaction of  $V^+$  with  $D_2O$ . *J. Phys. Chem.* **1994**, *98*, 7538-7544.
18. Clemmer, D. E.; Chen, Y.-M.; Khan, F. A.; Armentrout, P. B., State-Specific Reactions of  $Fe^+(a^6D, a^4F)$  with  $D_2O$  and Reactions of  $FeO^+$  with  $D_2$ . *J. Phys. Chem.* **1994**, *98*, 6522-6529.
19. Kickel, B. L.; Armentrout, P. B., Guided Ion Beam Studies of the Reactions of  $Ti^+$ ,  $V^+$ , and  $Cr^+$  with Silane. Electronic State Effects, Comparison to Reactions with Methane, and  $M^+-SiH_x$  ( $x = 0 - 3$ ) Bond Energies. *J. Am. Chem. Soc.* **1994**, *116*, 10742-10750.
20. Kickel, B. L.; Armentrout, P. B., Reactions of  $Fe^+$ ,  $Co^+$  and  $Ni^+$  with Silane. Electronic State Effects and  $M^+-SiH_x$  ( $x = 0 - 3$ ) Bond Energies. *J. Am. Chem. Soc.* **1995**, *117*, 764-773.

21. Kickel, B. L.; Armentrout, P. B., Guided Ion Beam Studies of the Reactions of Group 3 Metal Ions ( $\text{Sc}^+$ ,  $\text{Y}^+$ ,  $\text{La}^+$ , and  $\text{Lu}^+$ ) with Silane. Electronic State Effects, Comparison to Reactions with Methane, and  $\text{M}^+\text{-SiH}_x$  ( $x = 0 - 3$ ) Bond Energies. *J. Am. Chem. Soc.* **1995**, *117*, 4057-4070.
22. Kickel, B. L.; Armentrout, P. B., Guided Ion Beam Studies of the Reactions of  $\text{Mn}^+$ ,  $\text{Cu}^+$ , and  $\text{Zn}^+$  with Silane.  $\text{M}^+\text{-SiH}_x$  ( $x = 0 - 3$ ) Bond Energies. *J. Phys. Chem* **1995**, *99*, 2024-2032.
23. Chen, Y.-M.; Elkind, J. L.; Armentrout, P. B., Reactions of  $\text{Ru}^+$ ,  $\text{Rh}^+$ ,  $\text{Pd}^+$ , and  $\text{Ag}^+$  with  $\text{H}_2$ , HD and  $\text{D}_2$ . *J. Phys. Chem.* **1995**, *99*, 10438-10445.
24. Rue, C.; Armentrout, P. B.; Kretzschmar, I.; Schröder, D.; Harvey, J. N.; Schwarz, H., Kinetic-energy Dependence of Competitive Spin-allowed and Spin-forbidden Reactions:  $\text{V}^+ + \text{CS}_2$ . *J. Chem. Phys.* **1999**, *110* (16), 7858-7870.
25. Rue, C.; Armentrout, P. B.; Kretzschmar, I.; Schröder, D.; Schwarz, H., Guided Ion Beam Studies of the State-Specific Reactions of  $\text{Cr}^+$  and  $\text{Mn}^+$  with  $\text{CS}_2$  and  $\text{COS}$ . *Int. J. Mass Spectrom.* **2001**, *210/211*, 283-301.
26. Liyanage, R.; Armentrout, P. B., Ammonia Activation by Iron: State-Specific Reactions of  $\text{Fe}^+$  ( $^6\text{D}$ ,  $^4\text{F}$ ) with  $\text{ND}_3$  and the Reaction of  $\text{FeNH}^+$  with  $\text{D}_2$ . *Int. J. Mass Spectrom.* **2005**, *241*, 243-260.
27. Xu, Y.; Chang, Y.-C.; Ng, C.-Y., Chemical Activation of a Deuterium Molecule by Collision with a Quantum Electronic State-Selected Vanadium Cation. *J. Phys. Chem. A* **2019**, *123* (28), 5937-5944.
28. Chang, Y. C.; Xiong, B.; Xu, Y.; Ng, C.-Y., Quantum Spin–Orbit Electronic State Selection of Atomic Transition Metal Vanadium Cation for Chemical Reactivity Studies. *J. Phys. Chem. A* **2019**, *123* (12), 2310-2319.
29. Chang, Y. C.; Xu, Y.; Ng, C.-Y., Quantum state control on the chemical reactivity of a transition metal vanadium cation in carbon dioxide activation. *Phys. Chem. Chem. Phys.* **2019**, *21* (13), 6868-6877.
30. Frisch, M. J.; Trucks, G. W.; Schlegel, H. B.; Scuseria, G. E.; Robb, M. A.; Cheeseman, J. R.; Scalmani, G.; Barone, V.; Petersson, G. A.; Nakatsuji, H.; et al. *Gaussian 16, Revision A.03*, Gaussian, Inc.: Wallingford CT, 2016.
31. Halkier, A.; Helgaker, T.; Jørgensen, P.; Klopper, W.; Koch, H.; Olsen, J.; Wilson, A. K., Basis-set convergence in correlated calculations on Ne,  $\text{N}_2$ , and  $\text{H}_2\text{O}$ . *Chem. Phys. Lett.* **1998**, *286*, 243-252.
32. Halkier, A.; Helgaker, T.; Jørgensen, P.; Klopper, W.; Olsen, J., Basis-set convergence of the energy in molecular Hartree–Fock calculations *Chem. Phys. Lett.* **1999**, *302*, 437-446.
33. Gdanitz, R. J.; Cardoen, W.; Windus, T. L.; Simons, J., Very Large Scale Computations of the Free Energies of Eight Low-Lying Structures of Arginine in the Gas Phase. *J. Phys. Chem. A* **2004**, *108*, 515 – 518.
34. Rodgers, M. T.; Armentrout, P. B., A Critical Evaluation of the Experimental and Theoretical Determination of Lithium Cation Affinities. *Int. J. Mass Spectrom.* **2007**, *267*, 167-182.
35. van Koppen, P. A. M.; Kemper, P. R.; Bowers, M. T., Electronic State-Selected Reactivity of Transition Metal Ions:  $\text{Co}^+$  and  $\text{Fe}^+$  with Propane. *J. Am. Chem. Soc.* **1992**, *114*, 10941-10950.
36. Kramida, A.; Ralchenko, Y.; Reader, J.; Team, N. A., NIST Atomic Spectra Database (ver. 5.7.1), [Online]. Available: <http://physics.nist.gov/asd>. National Institute of Standards and Technology, Gaithersburg, MD.: 2012.



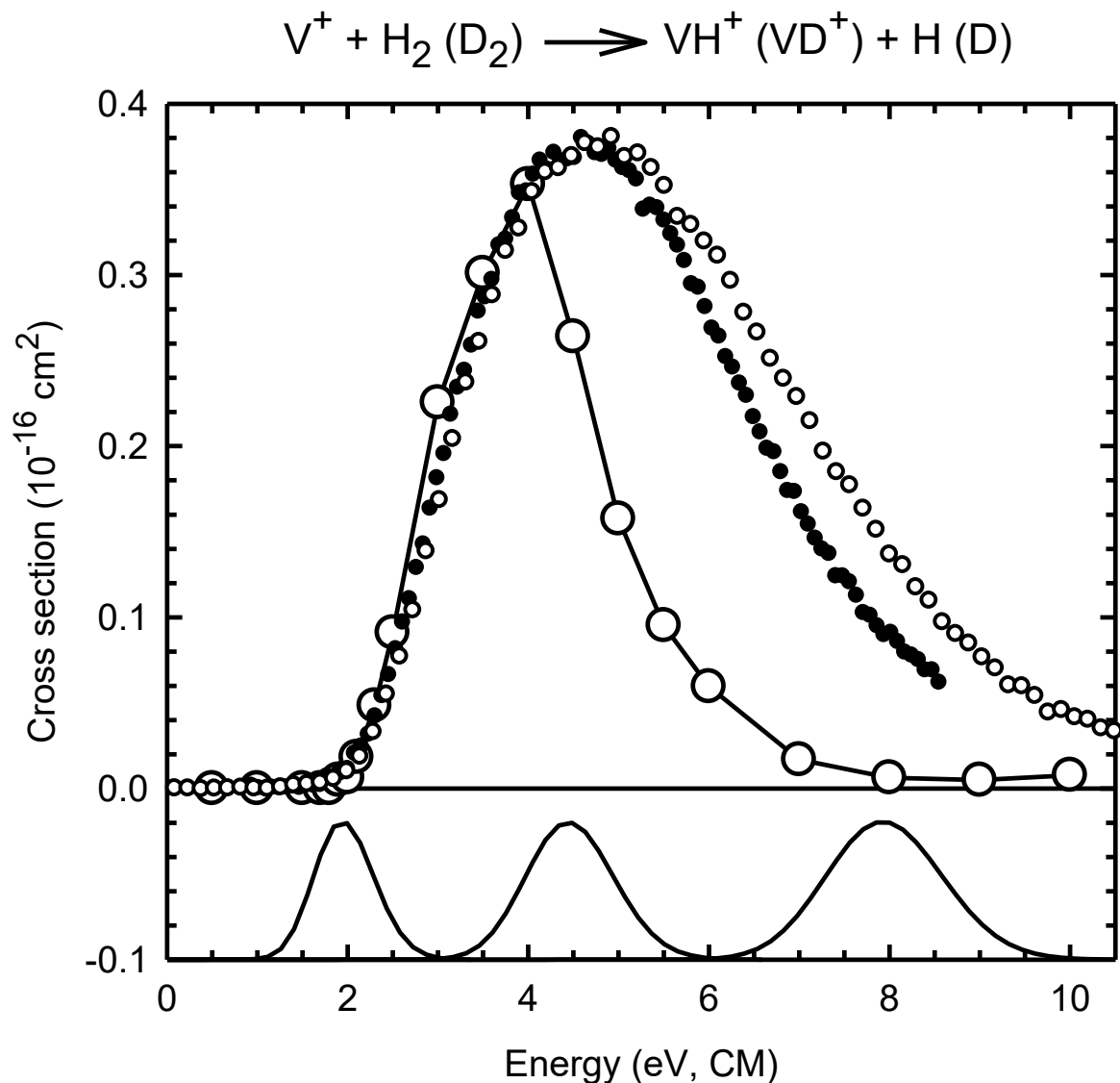
37. Ruscic, B.; Pinzon, R. E.; Laszewski, G. v.; Kodeboyina, D.; Burcat, A.; Leahy, D.; Montoy, D.; Wagner, A. F., Active Thermochemical Tables: Thermochemistry for the 21st Century. *Journal of Physics: Conference Series* **2005**, *16*, 561-570.
38. Ruscic, B.; Bross, D. H. Active Thermochemical Tables (ATcT) values based on ver. 1.122g of the Thermochemical Network. available at ATcT.anl.gov (accessed 4/29/20).
39. Chantry, P. J., Doppler Broadening in Beam Experiments. *J. Chem. Phys.* **1971**, *55*, 2746-2759.
40. Sunderlin, L. S.; Armentrout, P. B., Rotational Temperature Dependence of the Reaction of  $N^+$  and  $C^+$  with  $H_2$ , HD, and  $D_2$ . *J. Chem. Phys.* **1994**, *100*, 5639-5645.
41. Lifshitz, C.; Wu, R. L. C.; Tiernan, T. O.; Terwilliger, D. T., Negative Ion-molecule Reactions of Ozone and Their Implications on the Thermochemistry of  $O_3^-$ . *J. Chem. Phys.* **1978**, *68*, 247-260.
42. Eu, B. C.; Liu, W. S., On the Energy Dependence of Reaction Cross Sections Near Threshold. *J. Chem. Phys.* **1975**, *63* (1), 592-593.
43. Menzinger, M.; Yokozeki, A., On the Dynamical Content of Excitation Functions: Simple Linearization Procedures. *Chem. Phys.* **1977**, *22* (2), 273-280.
44. Morokuma, K.; Eu, B. C.; Karplus, M., Collision Dynamics and the Statistical Theories of Chemical Reactions. I. Average Cross Section from Transition-State Theory. *J. Chem. Phys.* **1969**, *51* (12), 5193-5203.
45. Chesnavich, W. J.; Bowers, M. T., Theory of Translationally Driven Reactions. *J. Phys. Chem* **1979**, *83* (8), 900-905.
46. Armentrout, P. B., The Kinetic Energy Dependence of Ion-Molecule Reactions: Guided Ion Beams and Threshold Measurements. *Int. J. Mass Spectrom.* **2000**, *200*, 219-241.
47. Armentrout, P. B., Not Just a Structural Tool: The Use of Guided Ion Beam Tandem Mass Spectrometry to Determine Thermochemistry. *J. Am. Soc. Mass Spectrom.* **2002**, *13*, 419-434.
48. Cheng, L.; Gauss, J.; Ruscic, B.; Armentrout, P. B.; Stanton, J. F., Bond Dissociation Energies for Diatomic Molecules Containing 3d Transition Metals: Benchmark Scalar-relativistic Coupled-cluster Calculations for Twenty Molecules. *J. Chem. Theor. Computation* **2017**, *13*, 1044-1056.
49. Chen, Y. M.; Clemmer, D. E.; Armentrout, P. B., Gas Phase Thermochemistry of VH and CrH. *J. Chem. Phys.* **1993**, *98*, 4929-4936.
50. Fang, Z.; Vasiliiu, M.; Peterson, K. A.; Dixon, D. A., Prediction of Bond Dissociation Energies/Heats of Formation for Diatomic Transition Metal Compounds: CCSD(T) Works. *J. Chem. Theory Comput.* **2017**, *13* (3), 1057-1066.
51. Ruscic, B.; Bross, D. H. Active Thermochemical Tables (ATcT) values based on ver. 1.122e of the Thermochemical Network. available at ATcT.anl.gov (accessed 10/15/19).
52. Weber, M. E.; Elkind, J. L.; Armentrout, P. B., Kinetic Energy Dependence of  $Al^+ + O_2 \rightarrow AlO^+ + O$ . *J. Chem. Phys.* **1986**, *84*, 1521-1529.
53. Safron, S. A.; Weinstein, N. D.; Herschbach, D. R.; Tully, J. C., Transition state theory for collision complexes: product translational energy distributions. *Chem. Phys. Lett.* **1972**, *12* (4), 564-568.
54. Sievers, M. R.; Armentrout, P. B., The Potential Energy Surface for Carbon-Dioxide Activation by  $V^+$ : A Guided Ion Beam Study. *J. Chem. Phys.* **1995**, *102*, 754-762.
55. Sievers, M. R.; Armentrout, P. B., Collision-Induced Dissociation Studies of  $V(CO)_x^+$ ,  $x = 1 - 7$ : Sequential Bond Energies and the Heat of Formation of  $V(CO)_6$ . *J. Phys. Chem* **1995**, *99*, 8135-8141.

Table 1. Modified line-of-centers models (eq 2) of SI data from EA and state-selected data from XCN.<sup>a</sup>

Reaction	$\sigma_0$	$n$	$E_0$ (eV)	$D_0(V^+-H)$
$V^+(SI) + H_2$	0.84 (0.17)	1.1 (0.1)	2.47 (0.05)	2.01 (0.05)
	<i>0.89 (0.18)</i>	<i>1.0 (0.1)</i>	<i>2.48 (0.05)</i>	<i>2.00 (0.05)</i>
$V^+(SI) + D_2$	0.58 (0.12)	1.2 (0.1)	2.45 (0.05)	2.07 (0.05) <sup>b</sup>
	<i>0.63 (0.13)</i>	<i>1.1 (0.1)</i>	<i>2.46 (0.05)</i>	<i>2.06 (0.05)<sup>b</sup></i>
$V^+(a^5D_2) + D_2$	1.35 (0.08)	1.0 (0.1)	2.41 (0.04)	2.12 (0.04) <sup>b</sup>
$V^+(a^5F_1) + D_2$	0.092 (0.011)	1.0 (0.1)	2.47 (0.08)	2.06 (0.08) <sup>b</sup>
$V^+(a^3F_2) + D_2$	5.1 (0.3)	1.1 (0.1)	2.44 (0.04)	2.08 (0.04) <sup>b</sup>

<sup>a</sup> In all cases,  $m = 1$ . Uncertainties (one standard deviation) in parentheses. For SI data, relative state reactivities are equal (roman) or 1 : 0.1 : 7 (*italic*) for  $a^5D$  :  $a^5F$  :  $a^3F$  states of  $V^+$ .

<sup>b</sup> Includes a zero-point vibrational energy correction of 0.03 eV.



**Figure 1.** Absolute integral cross sections for reaction of atomic vanadium cations with H<sub>2</sub> (solid symbols) or D<sub>2</sub> (open symbols) as a function of kinetic energy in the center-of-mass (CM) frame. Small symbols are taken from ref. 1 (EA) and correspond to V<sup>+</sup> formed by surface ionization (SI). Large symbols are taken from ref. 27 (XCN) and correspond to reactions of V<sup>+</sup> (*a*<sup>5</sup>D<sub>2</sub>) ions. Below the baseline, the Doppler profiles of the D<sub>2</sub> reaction are shown at 2.0, 4.5, and 8.0 eV.

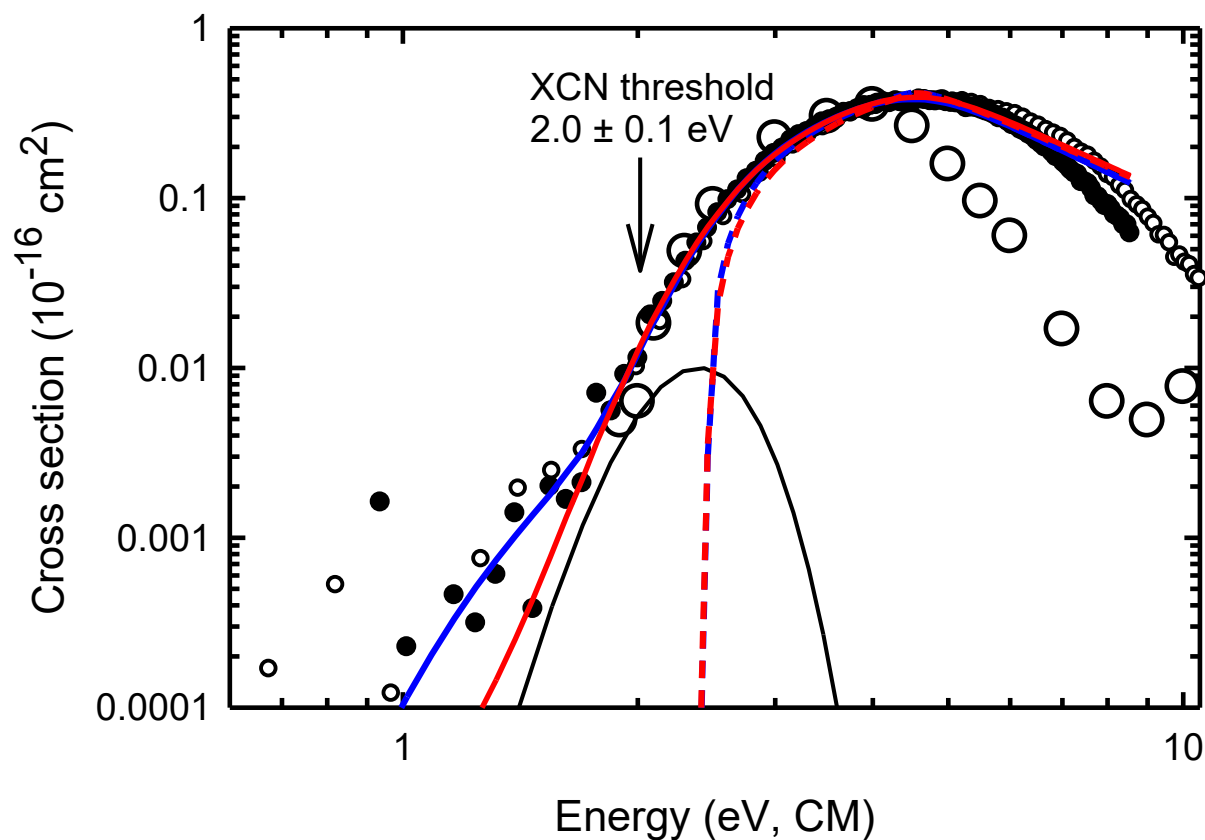


**Figure 2.** Same data as shown in Figure 1 now on log-log scales. The red and blue solid (dashed) lines show the modified line-of-centers (MLOC) model coupled with the probability of dissociation ( $P_D$ ) for the  $V^+ + H_2$  reaction of EA including (excluding) convolution with the electronic and kinetic energy distributions of the reactants. The red line assumes equal reactivity for all spin-orbit levels, whereas the blue line adopts the relative reactivities found by XCN, see text. The black line shows the Doppler profile of the  $H_2$  reaction at  $E_0 = 2.47$  eV. The arrow shows the data point chosen by XCN as their threshold energy.

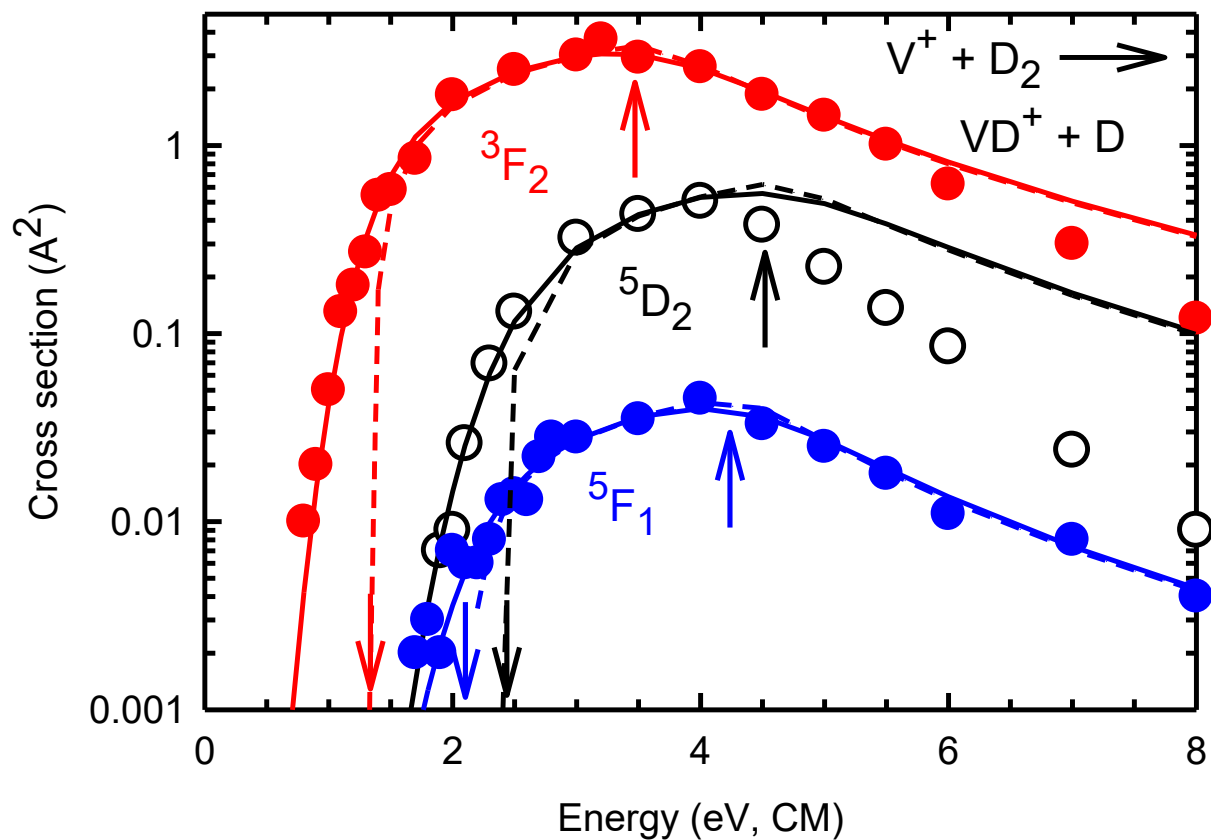


**Figure 3.** State-selected data (points) of XCN for reaction of D<sub>2</sub> with V<sup>+</sup>(*a*<sup>5</sup>D<sub>2</sub>) (black), V<sup>+</sup>(*a*<sup>5</sup>F<sub>1</sub>) (blue), and V<sup>+</sup>(*a*<sup>3</sup>F<sub>2</sub>) (red). The solid (dashed) lines show the modified line-of-centers (MLOC) models coupled with the probability of dissociation (P<sub>D</sub>) for each data set including (excluding) convolution with the kinetic energy distributions of the reactants. Vertical down arrows indicate the expected thresholds on the basis of the known excitation energies of each V<sup>+</sup> level and the best value for D<sub>0</sub>(V<sup>+</sup>-D) obtained in the present work. For P<sub>D</sub>, the onset for dissociation, E<sub>D</sub>, is fixed at D<sub>0</sub>(D<sub>2</sub>) – E<sub>e1</sub> (vertical up arrows) for all three electronic levels.

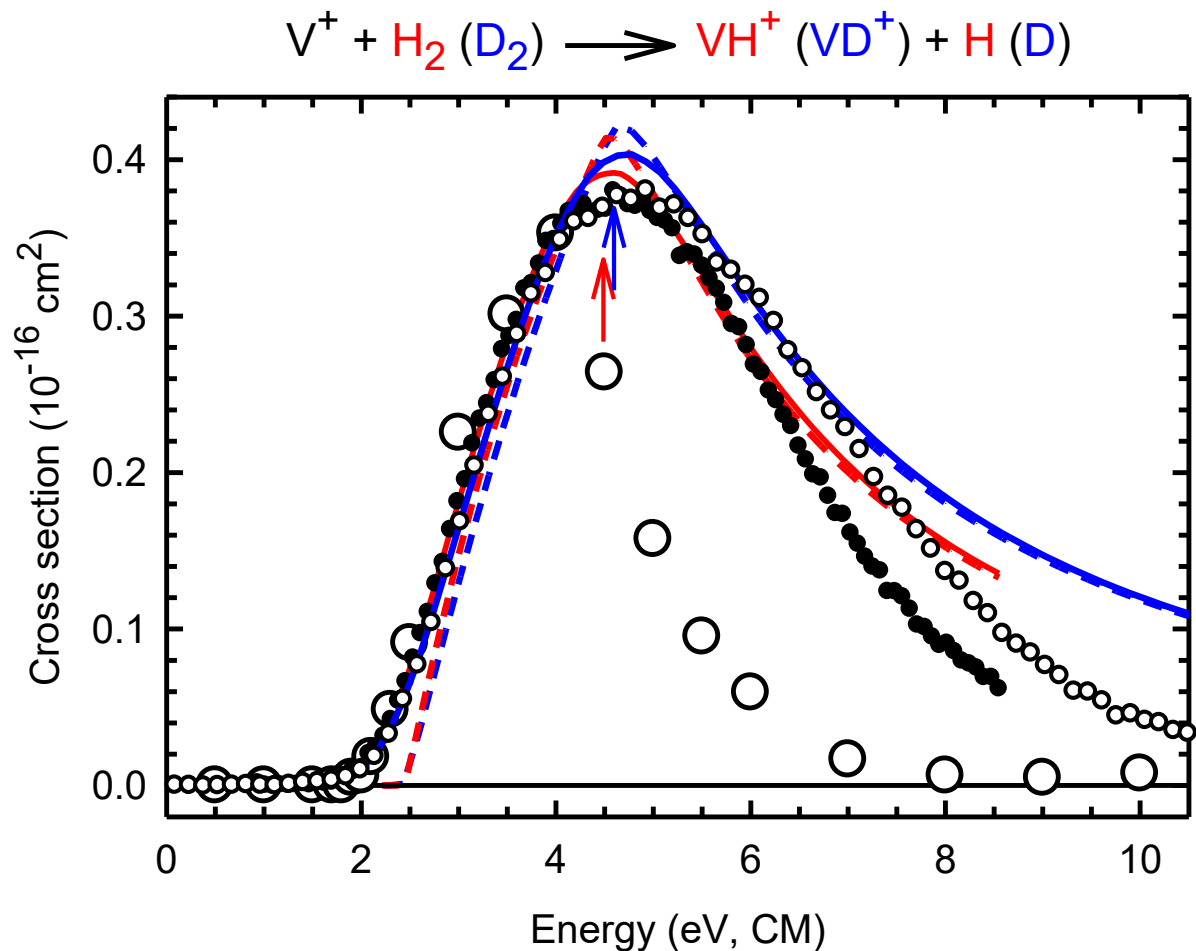


**Figure 4.** Same data as shown in Figure 1. The solid (dashed) lines show the modified line-of-centers (MLOC) model including the dissociation model ( $P_D$ ) for the  $\text{V}^+ + \text{H}_2$  (red) and  $\text{D}_2$  (blue) reactions of EA including (excluding) convolution with the electronic and kinetic energy distributions of the reactants. The onset for dissociation,  $E_D$ , is fixed at the bond energies of  $\text{H}_2$  at 4.478 eV and  $\text{D}_2$  at 4.556 eV as indicated by the arrows.

Table of Contents graphic

